Changes in Precipitating Snow Chemistry with Location and Elevation in the California Sierra Nevada

Jessie M. Creamean[1,2*†], Jessica L. Axson[3†], Amy L. Bondy[4], Rebecca L. Craig[4], Nathaniel W. May[4], Hongru Shen[3], Michael H. Weber[4], Kerri A. Pratt[4,5], and Andrew P. Ault[3,4*]

[1]Cooperative Institute for Research in Environmental Sciences, University of Colorado, Boulder, CO

[2]Physical Sciences Division, NOAA Earth System Research Laboratory, Boulder, CO

[3]Department of Environmental Health Sciences, University of Michigan, Ann Arbor, MI

[4]Department of Chemistry, University of Michigan, Ann Arbor, MI

[5]Department of Earth and Environmental Sciences, University of Michigan, Ann Arbor, MI

[*]Corresponding authors

[†]The authors contributed equally to this work

Contents of this file

Introduction

Supporting information includes supplementary text, figures, and tables that describe sample collection times, projected area diameters measured from Raman and SEM, additional details on the IC instrument including limits of detection (LODs), and comparison of our results with CARB $PM_{2.5}$ data.

Text S1. Sample Collection Times

Samples were collected during February and March 2013 for all three sites and an additional samples was collected for the TMD site in December 2012. Sampling start and stop times are given in Table S1.

Text S2. Measured Projected Area Diameters for Raman and SEM Dried Residues

To provide greater information on the size of particles analyzed by the Raman and SEM for these specific sample projected area diameter (d_{pa}) number size distributions for each sample are shown in Figure S1 and S2, respectively. For the Raman particles were primarily greater than 1 micron in diameter, with a mode between 1 and 2 microns. For the SEM particles ranged from 800 nm to 10 µm, a much wider range. The SEM sizes are larger than typical based on a combination of the specific instrument, the mode it was run in, and the samples themselves.

Text S3. Additional Details on the IC instrument

The ICS-1100 and ICS-2100 were equipped with Ultralow Pressure Trace Concentrator Columns for Reagent-Free IC (ICS-1100: IonPac TCC-ULP1 RFIC, 5 x 23mm, Dionex; ICS-2100: IonPac UTAC-ULP1 RFIC, 5 x 23 mm, Dionex), guard columns (ICS-1100: IonPac CG12A-5µm RFIC, 3 x 30 mm, Dionex; ICS-2100: IonPac AG18 RFIC, 4x50 mm, Dionex), analytical columns (ICS-1100: IonPac CS12A-5µm RFIC, 3x150 mm, Dionex; ICS-2100: IonPac AS18 RFIC, 4 x 250 mm, Dionex), suppressors (ICS-1100: CERS 500, 4 mm , ICS-2100: AERS 500, 4 mm, Dionex), and heated conductivity cells (DS6; Dionex). Limits of detection (LODs) are provided in Table S2.

Text S4. Comparison with CARB

Fine particulate mass concentrations ($PM_{2.5}$; µg m^{-3}) at Yosemite and sites downslope of Yosemite in the Central Valley (CV), were utilized to corroborate the potential regional sources of the insoluble residues with in the snow samples. Hourly $PM_{2.5}$ concentrations were acquired from the California Air Resources Board (CARB; http://www.arb.ca.gov/) sampling sites at the Yosemite Visitor Center (1222 m above mean sea level (AMSL); 37.75°N, 119.59°W), Modesto (33 m AMSL; 37.64°N, 120.99°W), Merced (56 m AMSL; 37.28°N, 120.43°W), and Madera (88 m AMSL; 36.95°N, 120.03°W). Hourly concentrations were averaged per sample during snow collection, in addition to concentration averages per day for the 2 days before collection of each sample to investigate CV pollutant trends prior to snowfall at Yosemite.
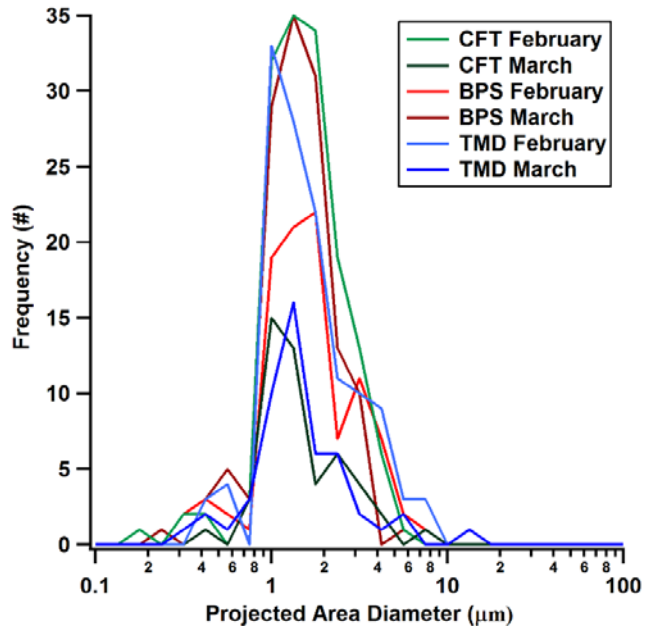
Figure S1. Raman measured projected area diameter (d_{pa}) number size distribution using 32 bins per decade showing a peak mode around 0.8 – 2 μm.
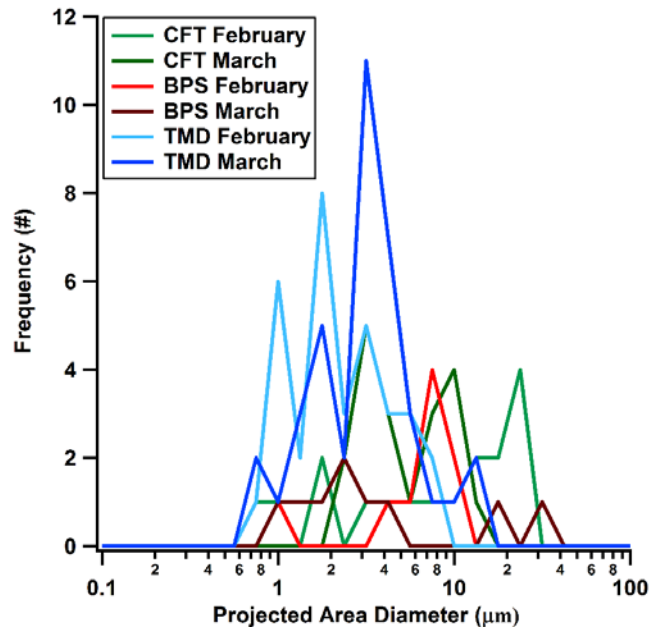

Figure S2. SEM measured projected area diameter using 8 bins per decade showing wide distribution ranging from 0.5 – 30 μm.
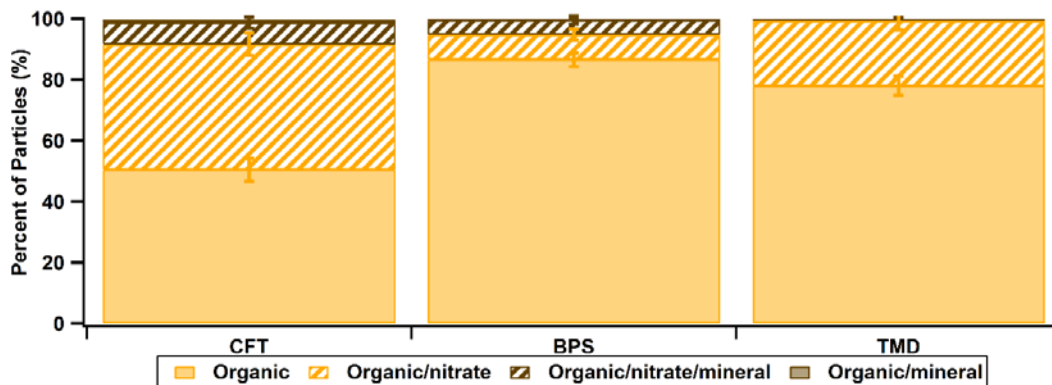
Figure S3. The average for all residue types observed using Raman microspectroscopy at the three sites over the two sampling periods.

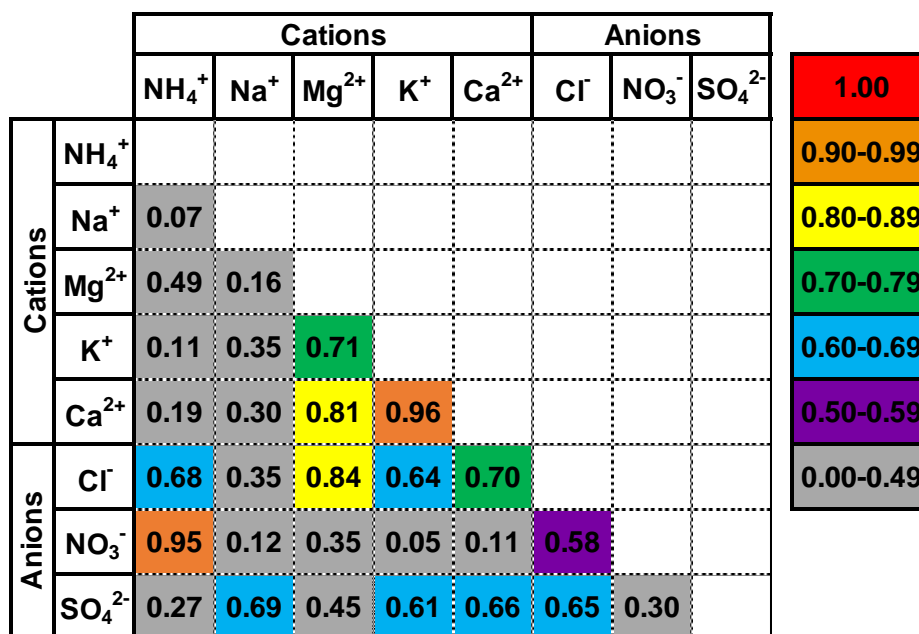|		Cations					Anions			Color scale
		NH_4^+	Na^+	Mg^{2+}	K^+	Ca^{2+}	Cl^-	NO_3^-	SO_4^{2-}	1.00
Cations	NH_4^+									0.90-0.99
	Na^+	0.07								0.80-0.89
	Mg^{2+}	0.49	0.16							0.70-0.79
	K^+	0.11	0.35	0.71						0.60-0.69
	Ca^{2+}	0.19	0.30	0.81	0.96					0.50-0.59
Anions	Cl^-	0.68	0.35	0.84	0.64	0.70				0.00-0.49
	NO_3^-	0.95	0.12	0.35	0.05	0.11	0.58			
	SO_4^{2-}	0.27	0.69	0.45	0.61	0.66	0.65	0.30		

Figure S4. Correlation coefficient matrix for concentrations of cations and anions from ion chromatography analysis of all Yosemite snow samples from all three collection sites. The color scale corresponds to the correlation coefficient.

Site	Start time (UTC)	End time (UTC)
Crane Flat (CFT)	19 Feb, 2013 16:45	20 Feb, 2013 15:40
	06 Mar, 2013 12:30	09 Mar, 2013 10:40
Badger Pass (BPS)	19 Feb, 2013 12:00*	20 Feb, 2013 12:00*
	08 Mar, 2013 12:00	09 Mar, 2013 12:10
Tuolumne Meadows (TMD)	17 Dec, 2012 10:00	18 Dec, 2012 08:05
	19 Feb, 2013 07:00	20 Feb, 2013 08:00
	06 Mar, 2013 14:25	07 Mar, 2013 09:00

Table S1. Snow sampling times for collection sites in Yosemite National Park. An asterisk indicates the sample where exact sampling start and end times were not recorded. These are estimated collection times.

Ion	LOD (μM)
Ammonium (NH_4^+)	2.35
Calcium (Ca^{2+})	1.05
Magnesium (Mg^+)	0.576
Potassium (K^+)	0.102
Sodium (Na^+)	6.74
Chloride (Cl^-)	0.705
Nitrate (NO_3^-)	2.82
Sulfate (SO_4^{2-})	1.46

Table S2. Limit of detection (LOD) for each cation and anion analyzed with ion chromatography.